SPATIAL CORRELATIONS OF THE GROUND MOTION RECORDED BY THE STRONG MOTION EARTHQUAKES INSTRUMENT ARRAY

Hidemori Narahashi (I)
Syun'itiro Omote (II)
Junji Maeda (III)
Morimasa Watakabe (IV)
Presenting Author: Hidemori Narahashi

SUMMARY

Spatial correlation of earthquake ground motions are investigated using cross-correlation coefficients and co-spectra (real part of coherences) between 18 digital accerelograms per an event recorded by the seismometers composing the sub-array station group of the Higashi-matsuyama local array (HMY), Japan. Tow-dimensional autoregressive model is applied to estimate the cross-correlation coefficients and co-spectra. It is concluded in this paper that horizontal heterogeneities of the shallower ground structure in the vicinity of the site as well as the kind of incident waves take dominant role to the spatial correlation of the ground motion during earthquakes.

INTRODUCTION

Digital records of the seismic arrays have opened a new way for promoting the wave analysis in the field of both seismology and earthquake engineering (Ref. 1, 2). Encouraged by the recommendations by IAEE New Delhi meeting in 1977, setting up of the seismic array stations has started in many seismic countries (Ref. 3). Using the digital records of the Higashi-matsuyama (HMY) local array, which belongs to a local arrays in the overall large array network system around Tokyo (Ref. 4), the spatial correlation of the ground motions during earthquake are investigated.

OBSERVATION SYSTEM AND DATA

As is shown in Fig. 1 the HMY local array network is consisted by six three-component sensors deployed three dimensionally. Four sensors, No. 2 to No. 5, were arranged horizontally in the area of 500m × 500m. The ground of the HMY site was composed by thick mudstone layer overleied by thin heterogeneous gravel layer having the thickness of 30 - 70m. Horizontally arranged four sensors were installed in the upper interface of the mudstone layer. Three sensors were arranged vertically, No. 6 on the ground, No. 2 playing a common sensor as horizontal and vertical arrays, in the depth of 60m and No.1 at the depth of 120m in the mudstone layer. In the following explanation, the location of the sensors is described as point 1, point 2 and so on. The mean velocities of P and S waves of the gravel layer are, after seismic prospecting,

(I) Research Associate, Kyushu Sangyo University, Fukuoka, Japan

(II) Professor, Kyushu Sangyo University, Fukuoka; Chairman of Research Committee of Strong-Motion Earthquake Instrument Arrays on Rock Sites

(III) Research Associate, Kyushu University, Fukuoka, Japan

(IV) Graduate Student, Kyushu University, Fukuoka, Japan

2km/s and 0.7km/s respectively, which are similar to the velocities of the mudstone. In this paper the digital data of two earthquakes are dealt with. One is the EQ No.323 on June 29, 1980 (M=6.7, h=10km) and the other is the EQ No.418 on Sep. 25, 1980 (M=6.1, h=80km). The radial directions from the foci of these earthquakes to the HMY site are also indicated in Fig. 1 by two arrows.

The spatial correlation of the ground motion are investigated on the bases of cross-correlation coefficients and normalized co-spectra calculated by the two-dimensional autoregressive estimation using the seismic records of vertical and horizontal sub-arrays. With regard to the vertical sub-array the cross-correlation coefficients and normarized co-spectra are worked out for the two combinations of point 6 and other points of the vertical array, on the other hand, with regard to horizontal sub-array these are worked out for the three combinations of point 2 and other points in horizontal sub-array, respectively. In addition, as it has been noticed, the spatial correlation is significantly influenced by the kind of waves, the calculations of correlation are worked out with respect to every wave group that is considered to belong the same wave types. As to the actual procedure, consulting with the obtained seismograms, under the appropriate judgement, grouping of wave types are carried out such as P, S and surface waves. The optimal order of the two dimensional autoregressive model determined by FPE criterion is 20 - 30 for all cases of combination and wave type in this paper.

THE THEORETICAL CORRELATION ON A SIMPLE DETERMINISTIC MODEL

In this section, we introduce a simple deterministic model for the ground structure, that is, the homogeneous semi-infinite space with the definite seismic wave velocities in order to examine the spatial correlation estimated from the ground motion records. In which case, it is reasonable for the HMY site to assume the wave velocity of 2.0km/s for P wave and 0.7km/s for S wave. Describing the auto-correlation coefficient and normalized power spectrum of the incident plane wave to the HMY site as "ρ" and "S", cross-correlation coefficients S_{ij} and co-spectra C_{oij} (real part of coherents) of the ground motions between the two points, point i (z_i, x_i) and point j (z_j, x_j), are derived as follows.

$$\rho_{ij}(\tau) = \frac{\rho(\tau' + \eta Z_1) + \rho(\tau' + \eta Z_2) + \rho(\tau' - \eta Z_2) + \rho(\tau' - \eta Z_1)}{2\sqrt{\{1 + \rho[2\eta(Z_1 + Z_2)]\}\{1 + \rho[2\eta(Z_1 - Z_2)]\}}} \qquad (1)$$

$$Co_{ij}(\omega) = \frac{\cos[\eta(Z_1 + Z_2)\omega/2]\cos[\eta(Z_1 - Z_2)\omega/2]}{|\cos[\eta(Z_1 + Z_2)\omega/2]||\cos[\eta(Z_1 - Z_2)\omega/2]|}\cos\zeta\omega X_2 \qquad (2)$$

where,

$\tau' = \tau - \zeta x_2$, $Z_1 = (z_j+z_i)/c$, $Z_2 = (z_j-z_i)/c$, $X_2 = (x_j-x_i)/c$

$\eta = \cos\theta$, $\zeta = \sin\theta$ θ; incident angle c; velocity of seismic wave

respectively. It may be convenient to establish the Cartesian coordinate of which origin is placed at the point 6 of the HMY local array with z-axis fixed vertically downward and x-axis variable to the radial direction from the epicenters to HMY site. When time-lag d_j is exist in the corss-correlation coefficients ρ_{2j} between point 2 and another point j (j=3, 4, 5) of horizontal sub-array, incident angle θ and apparent velocity v are estimated by the wellknown relations.

$$\theta = \sin(d_j/X_2) \qquad v = X_2/d_j \qquad \text{where,} \quad X_2 = (x_j-x_2)/c \qquad (3)$$

CORRELATION COEFFICIENTS AND COHERENCES OF THE GROUND MOTION ESTIMATED FROM THE DATA

In this chapter we like to extend our study in comparing and examining the cross-correlation coefficients and normalized co-spectra derived from two different ways, one is the result worked out from the observed earthquake data, and the other is the one derived theoretically from the model mentioned in the previous section. In the following description, in order to make clear the expression for the correlation estimated from the observed earthquake data, the notation "~" is employed. When identification of the wave type is needed a suffix (P, S, M) will be attached at the left bottom. In other cases when no confusion is expected the variable τ of the correlation coefficients and the variable ω of the co-spectra are sometimes omitted. All the following results are calculated for the definite duration time of waves, that is, 5.12sec for P, 7.68sec for S and 7.68sec for surface wave portions.

Correlation of P Waves

With regard to the P wave of the EQ No.323 and EQ No.418, the $\tilde{\rho}_j$ and $\tilde{S}_j$ (j=6, 2, 1) are shown in Fig. 2-1. In the like way the $\tilde{\rho}_{61}$ and $\tilde{C}_{61}$ are reproduced in Fig. 2-2. Firstly, refering to Fig. 2-1, it is worthy to note that the $\tilde{S}_6$ of the two earthquakes show quite a like figure for the frequency range 0 - 5Hz, in which fairly a high power exist, but not for the range 6 - 12Hz. This difference may give an indication that the incident P waves of the two earthquakes differed considerably in the frequency range higher than 5Hz. Secondly, the $\tilde{\rho}_{61}$ in Fig. 2-2 gave a clear peak at $\pm$0.06sec as was expected theoretically (Eq. 1), which lead us to consider that the P wave must have an incident path almost vertical. Quantitative estimation of the incident angle will be given in the next paragraph. Thirdly, the $\tilde{C}_{o61}$ in Fig. 2-2 shows that (i) the curves of the two earthquakes give little difference, (ii) quite a good accord is observed in the period range 0 - 8Hz between the observed curves and the one expected from the theoretical study, (iii) though the both two curves loss their conformity to the theoretical one in the frequency range higher than 8Hz, fairly large correlation between the two points, 6 and 1, still existing. Based upon these findings it can be derived following conclusions with respect to the site structures. (i) The ground structures covered by the HMY local array is physically stable. (ii) The assumption concerning with the array field which introduced in the previous section seems fairly reasonable to extend our deductions on the wave analysis in the limited frequency range (0 - 8Hz). (iii) It also seems that there is a good possibility to extend our wave analysis even in the more extended frequency range (0 - 35Hz), provided we could set up more improved ground structure model.

In Fig. 2-3 there are shown the $\tilde{\rho}_{2j}$ and $\tilde{C}_{o2j}$ (j=3, 4, 5) for the EQ No.323. Figures of the $\tilde{\rho}_{2j}$ and $\tilde{C}_{o2j}$ (j=3, 4, 5) calculated for the EQ No.418 are not reproduced here, but we obtained the same result as the case of the EQ No.323. As will be seen in Fig. 2-3 the first peaks of the $\tilde{\rho}_{2j}$ (j=3, 4, 5) give fairly large values of correlation coefficients such as 0.8 - 0.9 and time-lags of the first peaks are appeared. Time-lags indicate the time difference of the wave arrival at the point 2 and other points of horizontal sub-array, in that case "plus" time-lag shows earlier arrival at the point 2 than the others and "minus" value vice versa. Using these time-lags and the distance in the radial direction between horizontal sub-array points, the apparent propagation

velocity of the P wave and the incident angle to HMY site are calculated as $v = 11km/s$ and $\theta = 10°$ respectively. Consulting with C_{o2j} (j=3, 4, 5) in Fig. 2-3, it can be learned that the frequency range in which high correlation is existing is the range of 0 - 8Hz. It means that for the waves of which a quarter of a wave length is longer than 63m the correlation between the two points in the horizontal sub-array can be seen fairly clearly.

Correlation of S Wave among the Vertical Sub-array Points

Using the S wave parts of the two earthquakes of No.323 and No.418, the $\tilde{\rho}_j$ and $\tilde{S}_j$ (j=6, 2, 1) were calculated. Results are reproduced in Fig. 3-1. The ${}_s\tilde{\rho}_{61}$ and ${}_s\tilde{C}_{o61}$ are also reproduced in Fig. 3-2. The $\tilde{S}_6$ of EQ No.418 gives sharp peaks at the frequencies of 2, 5, 8 and 11Hz, while the peaks in EQ No.323 curve is hardly recognized. The $\tilde{\rho}_{61}$ in Fig. 3-2, shows a symmetrical curve against the time axis giving clear peaks on the both sides. In all S waves of both earthquakes, No.323 and No.418, and regardless in the difference of the components EW and NS, the time-lag of these peaks are ±0.17sec, which just coincide with the value expected from the model mentioned in the previous section. With regard to the $\tilde{C}_{o61}$ in Fig. 3-2, the curve shows quite a good harmony with one given by Eq. 2, only excepting the tendency that the correlation decreases as frequency increases.

If we follow the same consideration as was the case of the P wave, the wave length that shows rather higher correlation will be more than 60m. So in the case of S wave it comes that under the assumed velocity the frequency range can be limited in the range of 0 - 12Hz. As will be seen in Fig. 3-2 it can be observed that up to this range the $\tilde{C}_{o61}$'s keep fairly a good correlation.

Correlation of S Waves between the Horizontal Sub-array Points

The $\tilde{\rho}_{2j}$ and $\tilde{C}_{o2j}$ (j=3, 4, 5) calculated with the S waves of the EQ No.323 and EQ No.418 are reproduced in Figs. 3-3 and 3-4. The time-lag observed in the ${}_s\tilde{\rho}_{2j}$ (j=3, 4, 5) of the EQ No.323 is naturally larger than we observed in the P wave cross-correlation coefficients of the same earthquake (${}_p\tilde{\rho}_{2j}$ (j=3, 4, 5) in Fig. 2-3). Using the delay times observed in Fig. 3-3, the incident angle of S waves to HMY site and the apparent velocity were obtained by Eq. 3. They are: $\theta = 5° - 11°$ and $v = 3.5 - 6.9km/s$ respectively. As we have seen in the case of the P wave in the preceding section, there is fairly a good accordance with the theory in the frequency range of 0 - 12Hz. In the case of the S wave, however, as is shown in the ${}_s\tilde{C}_{o2j}$ (j=3, 4, 5) for the EQ No.323 (Fig. 3-3) the frequency range in which the high accordance can be observed is limited only in the range of 0 - 3Hz.

The results of the analysis with the EQ No.418 are extremely different from the case of EQ No.323. With regard to the EQ No.418, the first peaks of the $\tilde{\rho}_{24}$ and $\tilde{\rho}_{25}$ in Fig. 3-3 are seen in the "plus" side with large time-lags while that of the $\tilde{\rho}_{23}$ in the "minus" side with small time-lag, in spite of the locations of the point 3, 4 and 5 are distant about -450m, 70m and 90m from the point 2 respectively in the radial direction. If we assume that the S wave comes up to the observation points through the vertical wave path, such events as we observed above can never be taken place.

Now, examining more in detail, it can be pointed out that the above nature are seen clearly in the waves of NS component. In the case of the EQ No.418

the NS component was fairly coincided with the transverse direction for each sensor of the HMY local array network. Taking into considerations of all these findings it may be concluded that in the wavetrains of 7.68sec time which we designated a priori as S wave in this research there might have been a possibility that Love wave group has co-existed having fairly a large wave energy. Based upon the distance between the point 2 and point 4, which stands as the nearest station to point 2 in the radial direction, and the time delay observed in the $\tilde{\rho}_{24}$ curve, the propagation velocity of the predominant Love wave can be estimated as 0.18km/s.

The Correlation of Surface Wave Group

The analysis was carried out for the surface wave group. In this case correlation of ground motion are showing fairly large difference for these earthquakes. With regard to the EQ No.418, the curves of the ${}_{M}\tilde{\rho}_{61}$ and ${}_{M}\tilde{C}_{61}$ are showing somewhat like shape with those of P or S wave groups, but correlation are lower considerablly. On the other hand, the $\tilde{\rho}_{61}$, $\tilde{C}_{o61}$ of the EQ No.323 shown in Fig. 4-1 is fairly different from the ${}_{s}\tilde{\rho}_{61}$ and ${}_{s}\tilde{C}_{61}$ of the S wave group (Fig. 3-2). As it can be noticed clearly, time-lag of the ${}_{M}\tilde{\rho}_{61}$ becomes hardly recognized especially for the records of NS and UD components. In addition, time-lags of the $\tilde{\rho}_{2j}$ (j=3, 4, 5), in Fig. 4-2, are much larger comparing to the case of S wave. Combining the time-lag of $\tilde{\rho}_{24}$ and $\tilde{\rho}_{25}$ with the distance between the two sub-array stations, the apparent propagation velocity is estimated as 1.0km/s - 2.0km/s. Now consulting with the research (Ref. 5) which worked out the group velocity of Rayleigh waves based on the seismic structure of the site down to the depth of 1.3km, it may be considered that the waves mentioned above represent so-called Airy phase of the first and/or second mode of the Rayleigh waves.

DISCUSSION AND CONCLUDING REMARKS

By means of the mathematical calculation technics to work out the cross-correlation coefficients and normalized co-spectra, somewhat detailed study was carried out about the spatial correlation between the points of the HMY local array observation network.

Through such studies following conclusions were obtained. (1) The body waves (P wave and S wave) are arriving to the HMY station along the path almost vertically upwards. Consulting with the delay time of the cross-correlation coefficients calculated for the horizontal sub-arrays, it can be estimated that the incident angle to the station is less than 10°. (2) The seismic waves that can show a high correlation between the two points in the horizontal sub-array are only those waves as having longer wave length that is determined by 60m × 4. In which case 60m represents the thickness of the gravel layer that underlay around the HMY array site area. Such a wave length may be expressed in terms of frequency of P and S wave, as 0 - 8Hz for P wave, 0 - 3Hz for S wave. (3) It is considered that the clear explanation can be given for the correlations between the vertical sub-array points, within a limited frequency range, provided the vertical ground structures along the sub-array points could be known exactly. In the case of the vertical sub-array of the HMY station, the frequency range, within which the theoretical explanations can be given in the accuracy of 80% , using the vertical ground structure so far known to us will be up to the frequencies of 0 - 35Hz for P wave and 0 - 12Hz for S wave, which corresponds to the thickness of the gravel layer

which are just representing a quarter of the wave lengths in the gravel layer for P and S waves respectively. (4) In some cases, following the S waves sooner arrival of Rayleigh and/or Love waves are observed. Therefore, in discussing the correlation between the two points, the sub-surface ground structures of the site up to the depth of 1 - 2km become important items to be examined. Even in the case of surface waves, the frequency range in which the close correlation can be observed between horizontal sub-array points are limited by the thickness of the gravel layer, as was observed in the case of the body waves.

As was stated above, it is clearly observed that three dimensional correlations of the earthquake ground motions between the HMY array stations are affected not only by the types of seismic waves but also by the lateral heterogeneity of the gravel layers that are lying underneath the site area. In accordance with the progress of the construction technics in recent years, the structure having a huge horizontal dimension such as long span bridges, have become to be constructed on the ground showing considerable lateral heterogeneity. In designing such a long dimension structure, it is needless to say that the carefull attentions should be payed for the phase difference of the input earthquake force at the different part of the body of the structure, but at the same time, much more carefull considerations should be called upon to examine the effect of decrease of the correlation of the ground motions caused by the heterogeneity of the ground along the lateral direction of the long structures.

ACKNOWLEDGEMENT

The authors express their hearty thanks to the Research Committee of Strong-Motion Earthquake Instrumentation Arrays on Rock Sites, sponsored by 10 Electric Power Co. Japan, and the operation of the instrumentations is carried over by the Kajima Institute of Construction Technology.

REFERENCES

1) B. A. Bolt, Y. B. Tsai, K. Yeh and M. K. Hsu Earthquake eng. struct. dyn., Vol.10, pp.561-573 (1983).
2) C. H. Loh, J. Penzien and Y. B. Tsai Earthquake eng. struct. dyn., Vol.10, pp. 575-591 (1983)
3) W. D. Iwan (editor) Proc. of the International Workshop on Strong-Motion Earthq. Instrument Arrays (May, 1978, Honolulu, Hawaii).
4) S. Omote, K. Ohmatsuzawa and T. Ohta Proc. 7th WCEE, Vol.2, pp.41-48 (1980).
5) K. Muto, T. Ohta, T. Sugano, M. Miyamura and M. Motosaka Proc. third international earthq. microzonation conf. (1982, Seattle, USA), Vol.I of III, pp.507-518.

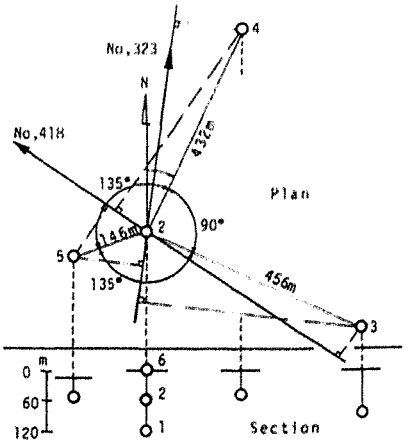

Fig. 1 A layout of the HMY local array network and the radial directions of No.323 and 418 earthquakes

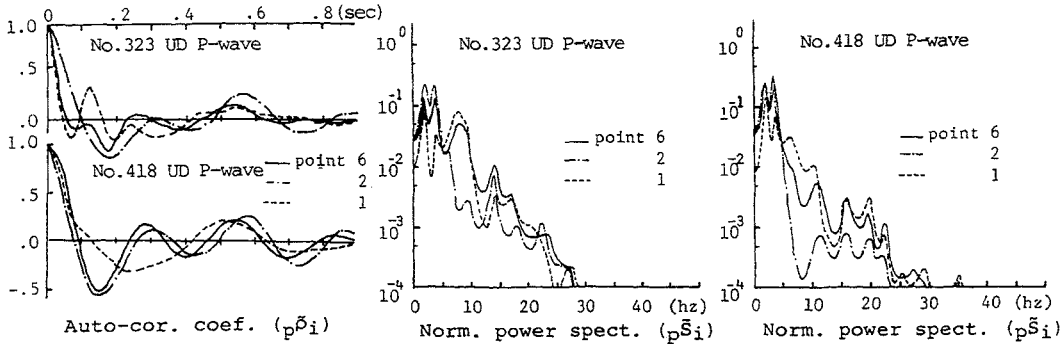

Fig. 2-1 Auto-correlation coefficients and normalized power spectra of the P wave motions at the three points belong to the vertical sub-array.

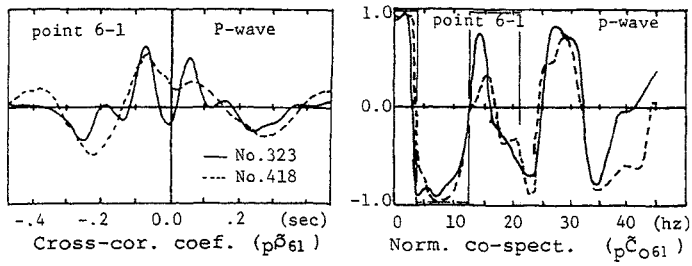

Fig. 2-2 Cross-correlation coefficients and normalized co-spectra of P wave motions between the point 6 and 1.

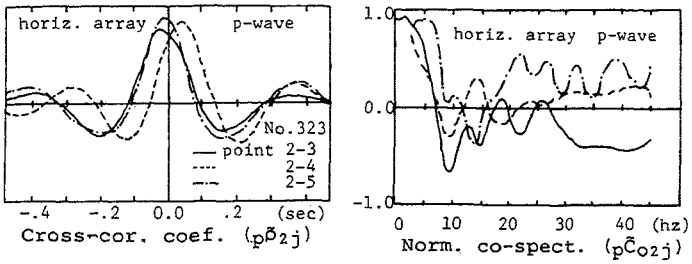

Fig. 2-3 Cross-correlation coefficients and normalized co-spectra of P wave motions during No.323 earthquake between the points of the horizontal sub-array.

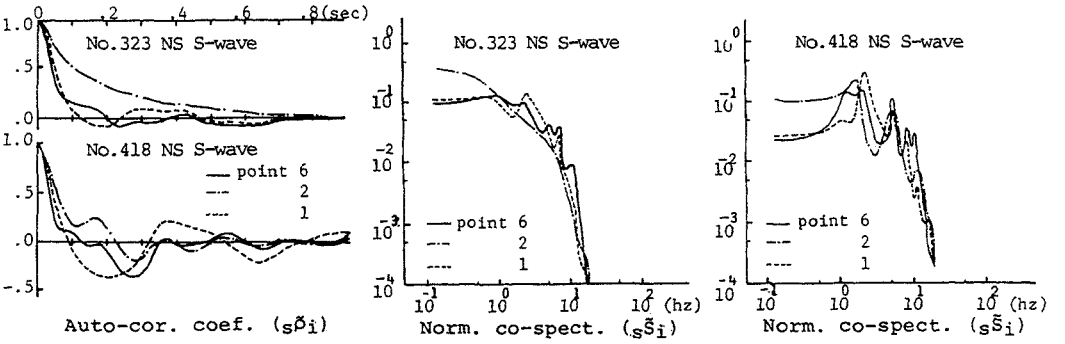

Fig. 3-1 Auto-correlation coefficients and normalized power spectra of the S wave motions at the three points belong to the vertical sub-array.

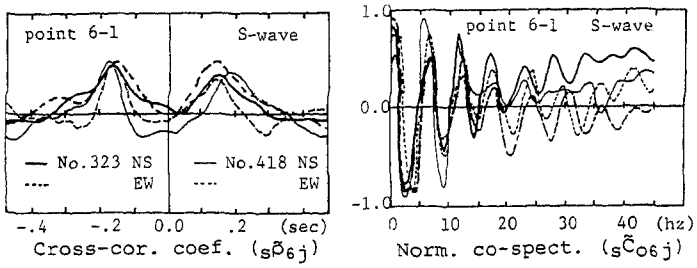

Fig. 3-2 Cross-correlation coefficients and normalized co-spectra of S wave motions between the point 6 and 1.

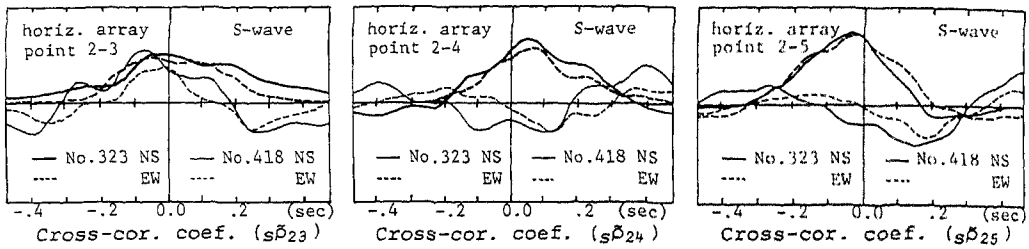

Fig. 3-3 Cross-correlation coefficients of S wave motions between the poitnt 2 and the others of the horizontal sub-array.

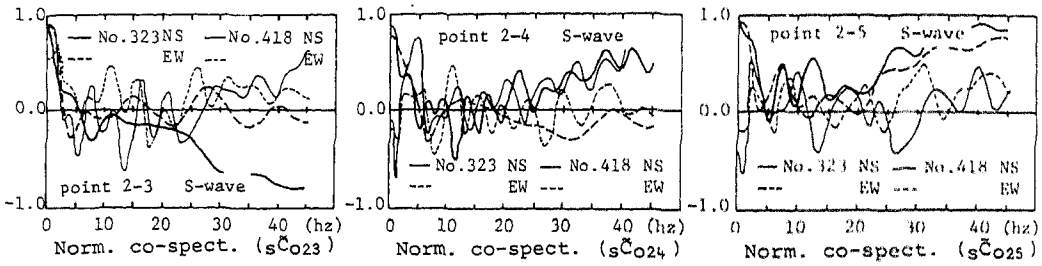

Fig. 3-4 Normalized co-spectra correspond to Fig.3-3.

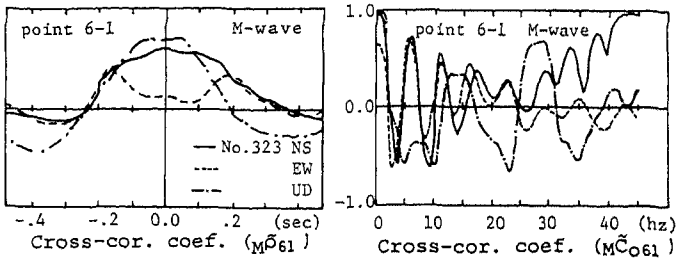

Fig. 4-1 Cross-correlation coefficients and co-spectra of surface wave type motion between point 6 and 1 during No.323 earthquake.

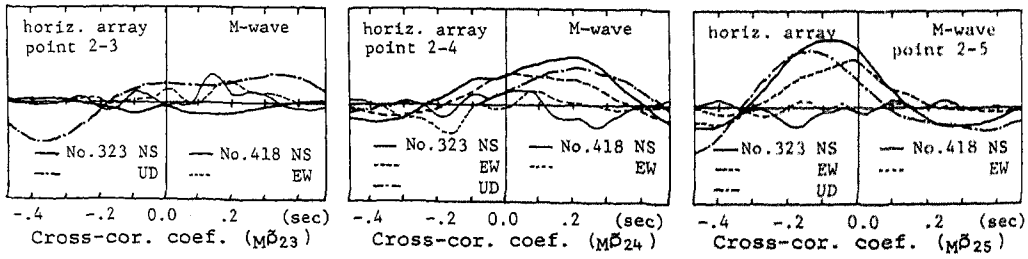

Fig. 4-2 Cross-correlations coefficients correspond to Fig. 4-1.